

**Ultrasound Speckle Reduction
Using Coded Excitation and Pulse Compression**

Project Proposal

By:

Josh Ullom

Project Advisor:

Prof. José Sánchez

Date:

December 1, 2009

Project Summary

Ultrasound images are riddled with system dependent imperfections called speckle (multiplicative noise). In ultrasonic imaging, detection of small lesions could be difficult because the effects of speckle may mask the visibility of these small targets. Therefore, the purpose of this project is to decrease speckle while maintaining some of the key salient features in the image. Images of tissue-mimicking phantoms will be created using Field II [1-2] in MATLAB (Natick, MA). Image quality metrics such as speckle signal-to-noise ratio (sSNR) [3] and contrast-to-noise ratio (CNR) [4] will be used to quantify improvements in image quality after various despeckling filters have been applied.

Project Description

The motivation of this study is to reduce speckle and improve image contrast while attempting to preserve key features in the image. The significance here lies in the improvement of diagnostic ultrasound imaging, which could potentially result in earlier detection of cancer.

In this study, two excitation methods will be used: conventional pulsing (CP) and a pre-enhanced chirp (REC). CP is the standard excitation used in most typical ultrasound devices. REC is a technique that improves axial resolution of the ultrasonic imaging system by a factor of 2 [5]. Recently, a technique known as REC-FC that combines the REC technique with frequency compounding (FC) was developed [6]. In this method, the spectrum of the radio frequency (RF) echo data was subdivided using subband filters to generate separate partially uncorrelated RF echoes. Consequently, these RF echoes were used to generate separate images that when compounded resulted in an image with reduced speckle. In the REC-FC study, various subband widths were evaluated. As the subband width became smaller, the variance in the image was reduced but at the expense of deteriorating the axial resolution. Therefore, the engineering tradeoff in REC-FC was contrast resolution vs. axial resolution.

A new technique known as enhanced REC-FC (eREC-FC) compounds several REC-FC images obtained at different subband widths. Contrary to REC-FC, with eREC-FC the contrast resolution was improved while maintaining an axial resolution comparable to CP [7]. However, with eREC-FC much of the speckle is still present in the image. Therefore, other speckle reduction techniques (despeckling filters) could be applied to reduce the speckle and improve the contrast even further. These filters include: local statistics, median, geometric, homomorphic deconvolution, anisotropic diffusion, and wavelet shrinkage.

Simulations and processing of experimental measurements will be performed utilizing MATLAB. Tissue-mimicking phantoms that simulate human tissue will be created in MATLAB so that ultrasonic images using CP and REC can be generated using Field II [1-2]. Field II [1-2] is an ultrasonic imaging add-on toolbox for MATLAB that could be used to simulate transducer field patterns and to generate accurate ultrasonic images. Once the images are generated, the despeckling filters will be applied to the CP and REC images. Finally, image quality metrics will be applied to quantify improvements in contrast and speckle reduction.

System Block Diagram

A processed image, $\hat{i}(x,y)$, results from applying a despeckling filter to the original image, $i(x,y)$, as seen in Fig. 1.

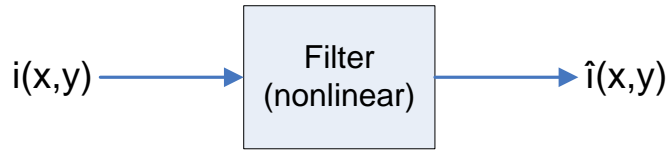


Fig. 1. General system block diagram.

Relevant Flowcharts

The basic idea behind REC is outlined in Fig. 2. By convolving the transducer's pulse-echo impulse response, $h_1(n)$, with a pre-enhanced chirp, $v_{PRE}(n)$, can be made to act as $h_2(n)$ convolved with a linear chirp, $v_{LIN}(n)$, resulting in $y(n)$. Basically, $h_1(n)$ responds like $h_2(n)$, which has more desirable characteristics, such as a larger bandwidth, which translates into improvements in axial resolution. Thus, $h_1(n) * v_{PRE}(n) = h_2(n) * v_{LIN}(n)$.

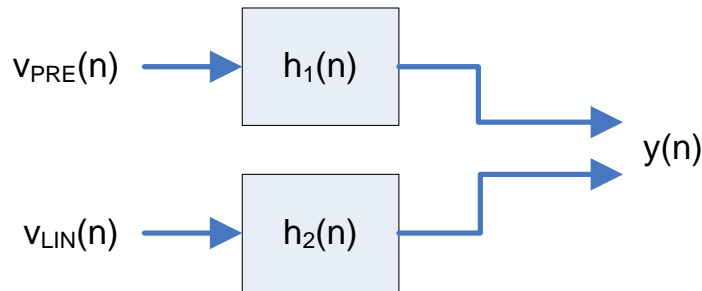


Fig. 2. Convolution equivalence

Images from tissue-mimicking phantoms will be created using Field II [1-2]. A simple guide for the creation of an image is shown in Fig. 3.

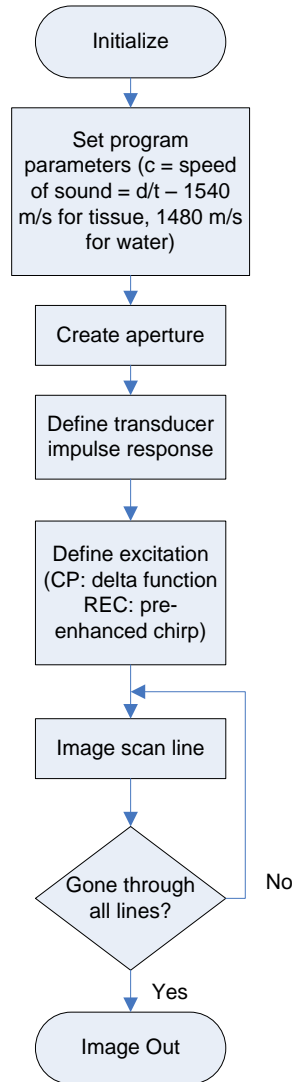


Fig. 3. Description of image creation using Field II [1-2].

Description of Filters

Local statistics filtering uses a moving window to compute local statistics, such as mean and variance, for pixels in a region-of-interest [8]. The equation to govern this process is [9]:

$$f_{i,j} = \bar{g}_{i,j} + k_{i,j} \cdot [g_{i,j} - \bar{g}_{i,j}],$$

where $f_{i,j}$ is the estimated pixel, $g_{i,j}$ is the middle pixel of the region-of-interest, $\bar{g}_{i,j}$ is the local mean value of the region contained by the window, and $k_{i,j}$ is a weighting factor described by

$k_{i,j} = \frac{\sigma^2}{\bar{g}_{i,j} \cdot \sigma^2 + \sigma_n^2}$, where σ is the variance in the window and σ_n is the noise variance in the window and $k \in [0 \ 1]$.

Median filtering takes the median of the pixels in the window and replaces the center pixel in a region-of-interest with that value and has the effect of removing spikes of noise [8,10].

Geometric filtering uses an iterative approach to make the central pixel more like the adjacent pixels [8,11].

Homomorphic deconvolution uses the FFT of the logarithmic compressed image, reduces noise by applying a despeckling filter, then calculates the inverse FFT of the image. The result is an image with sharper features and reduced speckle variation [8,12].

Anisotropic diffusion uses the classical isotropic diffusion equation to smooth the image in homogeneous region while preserving brightness at discontinuities. The image is altered by solving a nonlinear partial differential equation [8,13] that was proposed by Perona and Malik [14]:

$$\begin{cases} \frac{\partial I}{\partial t} = \text{div}[c(|\nabla I|) \cdot \nabla I] \\ I(t=0) = I_0 \end{cases}$$

where ∇ is the gradient vector, div is the divergence operator, $c(x)$ is the diffusion coefficient, $|x|$ stands for magnitude, and I_0 is the initial image. They go on to say to use two diffusion coefficients:

$$c(x) = \frac{1}{1 + \left(\frac{x}{k}\right)^2} \text{ and } c(x) = e^{-\left(\frac{x}{k}\right)^2}, \text{ where } k \text{ is an edge magnitude parameter.}$$

Wavelet shrinkage reduces speckle by filtering in the wavelet domain using the discrete wavelet transform [8,15].

Image Specifications

Speckle Signal-to-Noise Ratio (sSNR) – $sSNR = \frac{\mu}{\sigma}$ where μ is the mean and σ is the standard deviation of a homogeneous region in the image [3]. To have fully developed speckle, an ultrasonic image has a sSNR of 1.91 [16].

Contrast-to-Noise Ratio (CNR) – $CNR = \left| \frac{\mu_B - \mu_T}{\sqrt{\sigma_B^2 + \sigma_T^2}} \right|$ where μ_B is the brightness of the

background, μ_T is the brightness of the target lesion, σ_B^2 is the variance of the background, and σ_T^2 is the variance of the target [4]. CNR quantifies how well an object can be perceived compared to the surrounding background. The goal is to improve the CNR beyond the reference eREC-FC image after despeckling.

Preliminary Progress

A MATLAB function to generate tissue-mimicking phantoms has been created. The function allows the dimensions of the phantom, the diameter of the lesion in the phantom, and the scatterer density per resolution cell volume in the background and the lesion to be adjusted. A sample cylinder phantom is shown in Fig. 4.

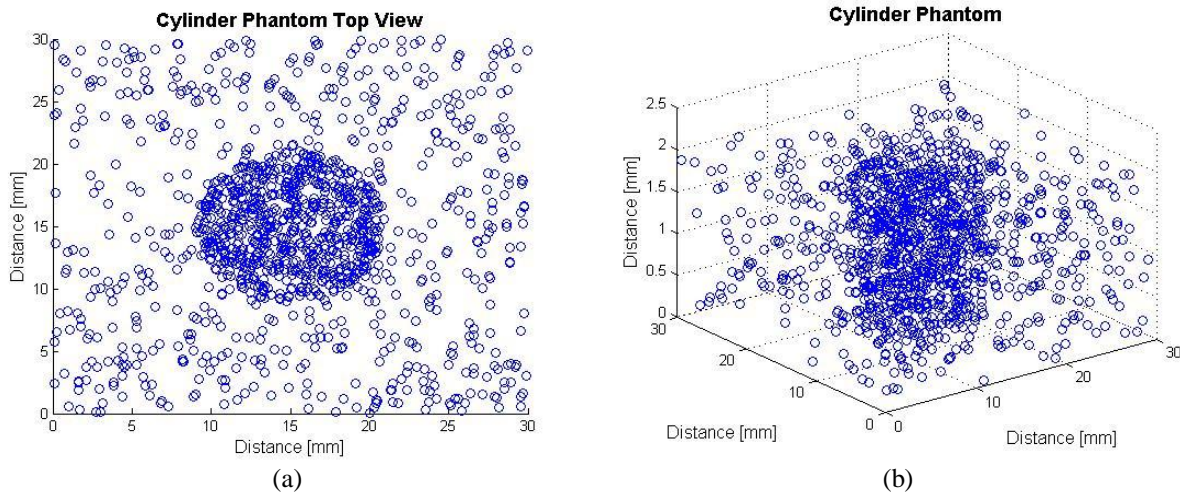


Fig. 4. MATLAB plots of a cylinder phantom with radius of 6 mm, a depth of 1 lateral beam width, and a scatterer density of 10 times the surrounding tissue to ensure visibility when viewing from (a) above the cylinder or (b) any 3-D angle

Software using Field II [1-2] to simulate phantoms using CP has been created, see Fig. 5.

3 Point Targets at Equal Depth

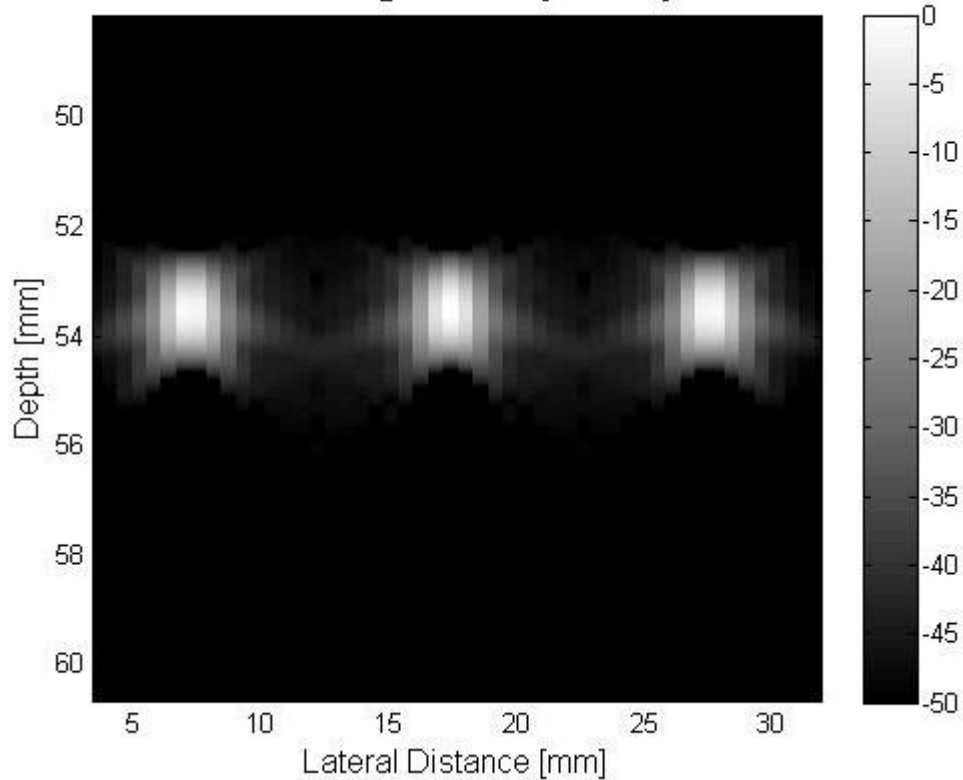


Fig. 5. Ultrasound image created using Field II [1-2] of point targets located at the focus of the source

The software implementation of the REC excitation scheme process is complete, and is shown graphically in Fig. 6 as an extension of Fig. 2. Fig. 7 shows the frequency analysis of Fig. 6 to further illustrate that the convolution of h_1 and v_{PRE} is equal to the convolution of h_2 and v_{LIN} .

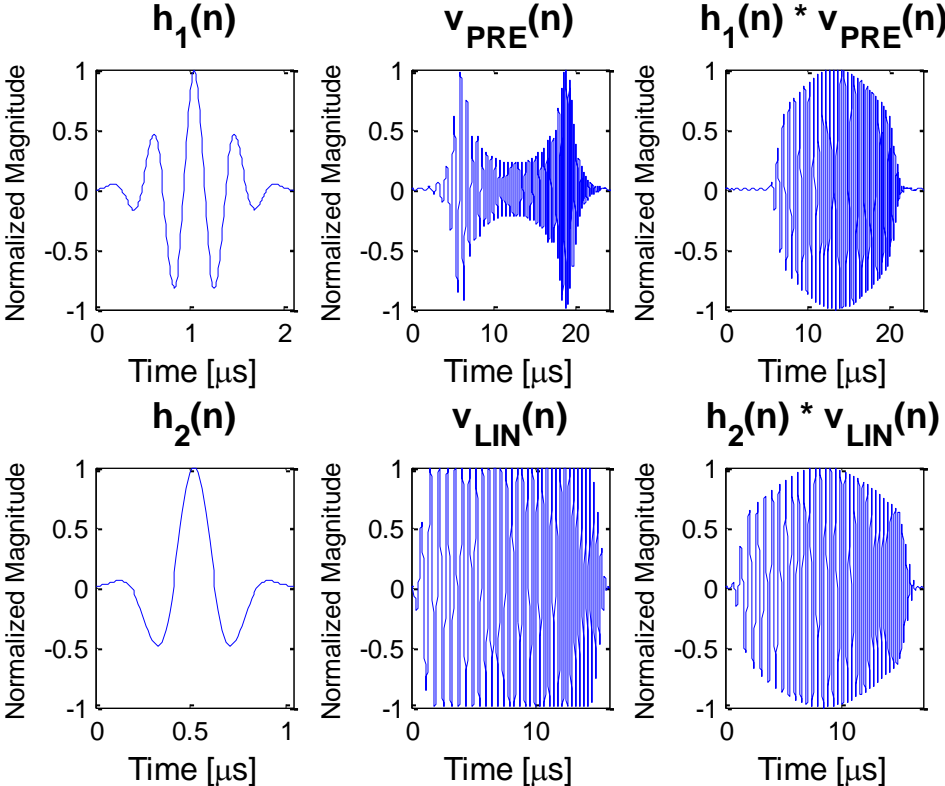


Fig. 6. MATLAB simulation of REC excitation scheme

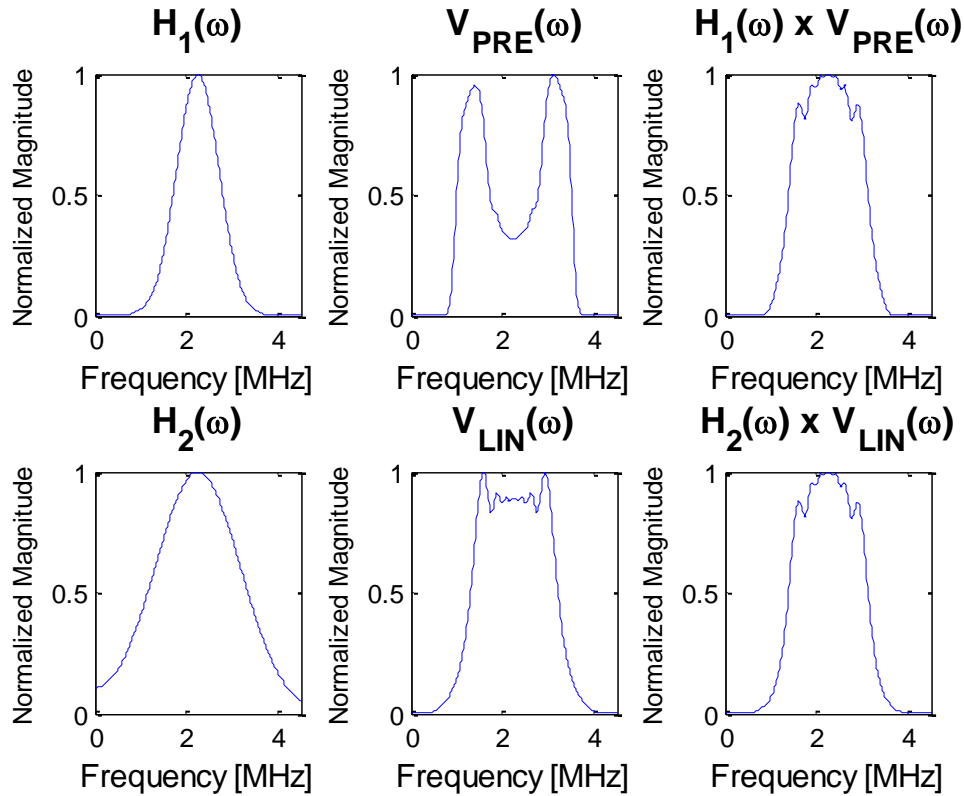


Fig. 7. Frequency Analysis of REC Excitation Scheme

Schedule

January 21, 2010	Median Filtering:	Research and Design
January 28, 2010		Implement and Quantify Results
February 4, 2010	Local Statistics Filtering:	Research and Design
February 11, 2010		Implement and Quantify Results
February 18, 2010	Geometric Filtering:	Research and Design
February 25, 2010		Implement and Quantify Results
March 4, 2010	Homomorphic Deconvolution:	Research and Design
March 11, 2010		Implement and Quantify Results
March 18, 2010	Anisotropic Diffusion:	Research and Design
March 25, 2010		Implement and Quantify Results
April 1, 2010	Wavelet Shrinkage:	Research and Design
April 8, 2010		Implement and Quantify Results
April 15, 2010	Finalize all work and begin final report	
April 22, 2010	Continue working on report and work on presentation	
April 29, 2010	Finalize report and finish presentation	
May 6, 2010	Final presentation	

Fig. 8. Project schedule

Patents

A search for patents was made and revealed that there was a patent application for utilizing REC-FC which has the application number 20090209858 and is titled “System and method for ultrasonic image processing” by Dr. Michael L. Oelze. This was incorporated into a previous U.S. Provisional Patent Application, Ser. No. 61/029,479, filed Feb. 18, 2008, by Dr. Oelze, entitled “Ultrasonic Imaging Speckle Suppression and Contrast Enhancement Technique.”

Equipment List

In order to facilitate the project’s continual progress, a computer dedicated solely to this project will be used. The computer is a Dell Optiplex 760, Round Rock, Texas, which has a quad-core, 64-bit processor and 4 GB of RAM. The software necessary for completing the project would be MATLAB and Field II [1-2].

References

- [1] J. A. Jensen. “Field: A program for simulating ultrasound systems,” *Medical & Biological Engineering & Computing*, Vol. 34, suppl. 1, pt. 1, pp. 351-353, 1996.
- [2] J. A. Jensen and N. B. Svendsen. “Calculation of pressure fields from arbitrarily shaped, apodized, and excited ultrasound transducers,” *IEEE Trans. Ultrason., Ferroelectr. Freq. Contr.*, vol. 39, no. 2, pp. 262-267, Mar. 1992.
- [3] S. W. Smith, R. F. Wagner, J. M. Sandrik, and H. Lopez. “Low contrast detectability and contrast / detail analysis in medical ultrasound,” *IEEE Trans. Sonics Ultrason.*, vol. 30, pp. 164-173, May 1983.
- [4] M. S. Patterson and F. S. Foster. “The improvement and quantitative assessment for B-Mode images produced by an annular array / cone hybrid,” *Ultrason. Imag.*, vol. 5, no. 3, pp. 195-213, Jul. 1983.
- [5] M. L. Oelze, “Bandwidth and resolution enhancement through pulse compression,” *IEEE Trans. Ultrason., Ferroelectr. Freq. Contr.*, vol. 54, no. 4, p. 770, Apr 2007.
- [6] J. R. Sanchez and M. L. Oelze, “An ultrasonic imaging speckle-suppression and contrast enhancement technique by means of frequency compounding and coded excitation,” *IEEE Trans. Ultrason. Ferroelectr. Freq. Control*, vol. 56, pp. 1327-1339, Jul. 2009
- [7] J. R. Sanchez, “Improving ultrasound imaging using novel coded excitation techniques,” Ph.D. dissertation, University of Illinois at Urbana-Champaign, Urbana, IL, USA, 2010.

- [8] C. P. Loizou, C. S. Pattichis, C. I. Christodoulou, R. S. H. Istepanian, M. Pantziaris, and A. Nicolaides. "Comparative evaluation of despeckle filtering in ultrasound imaging of the carotid artery," *IEEE Trans. Ultrason., Ferroelectr. Freq. Contr.*, vol. 52, no. 10, pp. 1653-1668, Oct. 2005.
- [9] C. P. Loizou, C. Christodoulou, C. S. Pattichis, R. Istepanian, M. Pantziaris, and A. Nicolaides. "Speckle reduction in ultrasound images of atherosclerotic carotid plaque," *14th International Conference on Digital Signal Processing, 2002*, vol. 2, pp. 525-528, 2002.
- [10] M. O. Ahmad and D. Sundararajan, "A fast algorithm for two-dimensional median filtering," *IEEE Trans. Circuits and Syst.*, vol. CAS-34, no. 11, pp. 1364-1374, Nov. 1987.
- [11] L. J. Busse, T. R. Crimmins, and J. R. Fienup, "A model based approach to improve the performance of the geometric filtering speckle reduction algorithm," *IEEE Ultrason. Symposium*, pp. 1353-1356, 1995.
- [12] S. Solbø and T. Eltoft, "Homomorphic wavelet-based statistical despeckling of SAR images," *IEEE Trans. on Geosci. Remote Sens.*, vol. 42, no. 4, pp. 711-721, Apr. 2004.
- [13] Y. Yu and S. T. Acton, "Speckle reducing anisotropic diffusion," *IEEE Trans. Image Process.*, vol. 11, no. 11, pp. 1260-1270, Nov. 2002.
- [14] P. Perona and J. Malik, "Scale space and edge detection using anisotropic diffusion," *IEEE Trans. Pattern Anal. Machine Intell.*, vol. 12, pp. 629-639, 1990.
- [15] X. Zong, A. F. Laine, and E.A. Geiser, "Speckle reduction and contrast enhancement of echocardiograms via multiscale nonlinear processing," *IEEE Trans. Med. Imag.*, vol. 17, no. 4, pp. 532-540, Aug. 1998.
- [16] C. Burckhardt, "Speckle in ultrasound B-Mode scans," *IEEE Trans. Sonics Ultrason.*, vol. SU-25, pp. 1-6, Jan. 1978.